24th COBEM - 2017

24th ABCM International Congress of Mechanical Engineering
December 3-8, 2017, Curitiba, PR, Brazil

COBEM-2017-0796
EXPERIMENTAL IDENTIFICATION OF UNBALANCE AND SHAFT BOW IN A LAVAL ROTOR BY MEANS OF CORRELATION ANALYSIS AND MODEL ORDER REDUCTION

Fabio Dalmazzo Sanches[1]
Robson Pederiva[2]
[1] *Department of Mechanical Engineering, Federal University of Rio Grande do Norte, Technology Center, Natal 59078-970, RN, Brazil.*
[2] *Faculty of Mechanical Engineering, University of Campinas, Cidade Universitária Zeferino Vaz, Campinas 13083-860, SP, Brazil.*
dalmazzo@ct.ufrn.br, robson@fem.unicamp.br

Abstract. *This paper discusses the experimental identification of the simultaneous occurrence of two of the most common faults in rotors: unbalance and shaft bow, which present similar symptoms. Thus the faults identification becomes a challenging matter. The dynamic system was modeled by finite elements and the bearing parameters as well as the damping system were determined by differential evolution optimization technique. The faults were identified, both in magnitude and location (phase) using correlation analysis of the rotor outputs measured at the disc linear degrees of freedom. In order to avoid computational costs, Guyan order reduction method was employed and the identification used the reduced rotor model. Several experiments were performed considering different unbalance configurations and the proposed procedure proved consistent in identifying two faults that occur simultaneously and have similar symptoms.*

Keywords: *Faults identification, Correlation analysis, Model order reduction, Rotor dynamics*

1. INTRODUCTION

Faults in rotating machines are common and can cause several troubles such as financial losses, low performance, unsafe operation, etc.

The most common fault is probably unbalance, since there is no such thing as a perfectly balanced machine. Errors of geometric dimensions, mounting, and raw material inhomogeneity make it difficult to have a perfectly balanced object, since they cause undesirable vibrations that can affect machine performance. Lal and Tiwari (2012) state that estimating unbalance is a long-standing problem, but research in this field is still active. Markert, Platz and Seidler (2001) propose a model based method in time domain. The faults can be modeled as a set of equivalent forces and moments that generate the observed dynamic behavior. Least squares fitting and the concept of residuals, defined by the difference between the vibrations of the damaged system and the normal vibrations of the undamaged system, have been used to identify unbalance and rubbing.

Pennacchi et al. (2006) adopt residuals and least squares fitting in the frequency domain, as well as the foundation model, to generate algorithm able to identify the unbalance. The authors also present the mathematical modeling of the following faults: rotor bow, rigid coupling misalignment, transverse crack and journal ovalisation.

Jain and Kundra (2004) adopted the methodology proposed by Markert, Platz and Seidler (2001) in the theoretical estimation of unbalance and transverse fatigue cracking of the shaft, but these faults were considered separately. Jalan and Mohanty (2009) used the same technique to identify unbalance in the presence of misalignment. Lal and Tiwari (2012) developed an identification algorithm based on least-squares fitting for the simultaneous estimation of dynamic bearing parameters, residual unbalances and misalignment of a rigid turbine-generator. Tiwari and Chougale [12] used least-squares fitting to estimate the unbalance and the physical magnetic bearing parameters. Chatzisavvas and Dohnal (2015) applied the Least Angle Regression (LAR) technique to identify unbalance parameters.

Another common fault in rotating machines, which may be permanent or temporary, is the shaft bow that occurs when the shaft sags due to gravity, thermal distortions caused by asymmetric heating or cooling, and mechanical bow due to unbalance, for example.

Nicholas, Gunter and Allair (1976) published a pioneering work about shaft bow response in a Laval rotor. They demonstrated that the dynamic behavior of a bowed rotor differs from that caused by unbalance, and described the self balancing phenomenon that occurs when the shaft bow is 180° out of phase with the disk unbalance.

Shiau and Lee (1989) studied the effect of residual shaft bow on the dynamic response of a simply supported single disk rotor with disk skew and mass unbalances. Rossner, Thuemmel and Ulbrich (2015) used the Ritz approach enriched with specific shape functions to identify bow, unbalance and roundness separately via optimization of the rotor orbital parameters. Sanches and Pederiva (2011) identified unbalance and shaft bow theoretically for a two-piece disk rotor, using a simple mathematical model of the rotor based on the lumped mass matrix.

This paper presents the experimental identification of the magnitude and location (phase) of unbalance and shaft bow that occur simultaneously. The tests are done in a test rig, considering four different changes in the location of unbalance, allowing for the verification of different combinations of unbalance angular positions and the shaft bow.
The identification algorithm, proposed by Pederiva (1992), is performed in the time domain and is based on the mathematical modeling of the rotor and the faults, which are determined using only the rotor responses without trial runs. The Guyan reduction is applied to reduce the order of the rotor model, so that the responses of proximity probes can be used in the disk position, without using trial runs.

2. BRIEF THEORETICAL BACKGROUND

In general, a model composed of beam Finite Elements is used to describe the mechanical properties of the shaft while the dynamics effects caused by the bearings are modeled by means of a widely used approach considering a linear load-deflection relationship between the forces acting on the shaft due to the bearing and the resultant displacements and velocities of the shaft. Then, the equation of motion of the rotating machine can be expressed in the following general form:

$$[M]\{\ddot{\xi}(t)\}+[P]\{\dot{\xi}(t)\}+[K]\{\xi(t)\}=[H]\{n_{un}(t)\}+[B]\{n_b(t)\} \tag{1}$$

where $[M]$ is the mass matrix, $[P]$ is the force proportional to velocity matrix, which contains the damping and gyroscopic matrices, and $[K]$ is the force proportional to displacement matrix; all previously mentioned matrices have order (n,n). $\{\ddot{\xi}(t)\}$, $\{\dot{\xi}(t)\}$ and $\{\xi(t)\}$ are the vectors of acceleration, velocity and displacement, respectively whose orders are equal to g and contain the translational and rotational degrees of freedom. $[H]$ is the unbalance matrix and $[B]$ is the shaft bow matrix whose orders are (n,p). $\{n_{un}(t)\}$ and $\{n_b(t)\}$ are input vectors of unbalance and shaft bow, respectively and have order p.

The unbalance force is modeled as a force that is present in a given location in the rotor, which coincides with the disk position, since the disk is considered the source of unbalance (Lalanne and Ferraris, 1990):

$$\begin{Bmatrix} 0 \\ \vdots \\ F_u \\ F_w \\ 0 \\ \vdots \\ 0 \end{Bmatrix} = \begin{bmatrix} 0 & 0 \\ \vdots & \vdots \\ m_u d\Omega^2 & 0 \\ 0 & m_u d\Omega^2 \\ 0 & 0 \\ \vdots & \vdots \\ 0 & 0 \end{bmatrix} \begin{Bmatrix} \sin(\Omega t+\beta) \\ \cos(\Omega t+\beta) \end{Bmatrix} \tag{2}$$

where m_u is the unbalanced mass, d is the eccentricity, Ω is the rotor running speed and β is the unbalance phase angle..

The bow is modeled as elastic force acting on the shaft (Nicholas, Gunter and Allair, 1976). Since the shaft stiffness matrix derives from the finite elements, the bow is distributed over all the shaft nodes:

$$\{F_b\}=[K]\{\delta\} \tag{3}$$

and

$$\{\delta\} = \begin{Bmatrix} \delta_i \sin(\Omega t + \alpha_i) \\ \delta_i \cos(\Omega t + \alpha_i) \\ \delta_{ai} \cos(\Omega t + \alpha_i) \\ -\delta_{ai} \sin(\Omega t + \alpha_i) \end{Bmatrix} \tag{4}$$

where δ_i represents the linear bow caused by shaft deflection at the i^{th} shaft node, δ_{ai} is the angular bow caused by shaft arching, which is presented in the rotational degrees of freedom of the finite elements model, and α_i is the shaft bow phase.

Figure 1 shows a schematic diagram of the bow.

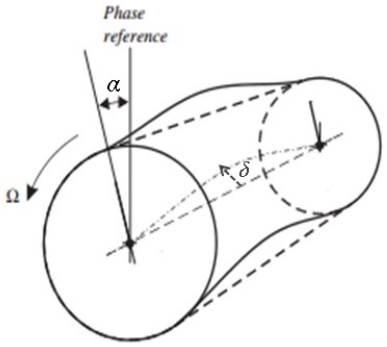

Fig. 1 – Schematic diagram of the shaft bow

Representation of state space

The rotor-bearing system described by Eq.(1) can also be described by the well-known state-space representation:

$$\{\dot{x}(t)\}_{(2n,1)} = [A]_{(2n,2n)}\{x(t)\}_{(2n,1)} + ([E_u] + [E_b])_{(2m,2)} \begin{Bmatrix} \sin(\Omega t) \\ \cos(\Omega t) \end{Bmatrix} = [A]\{x(t)\} + [E]\{n(t)\} \tag{5}$$

Details about the matrices $[A]$, $[E_u]$ and $[E_b]$ can be seen in details in Sanches (2015). The subscripts u an b mean the unbalance and bow, respectively.

The correlation matrix is defined by:

$$[R_{xx}(t, t+\tau)] = [R_{xx}(\tau)] = \varepsilon\{\{x(t)\}\{x^T(t+\tau)\}\} \tag{6}$$

where ε represents the expected value between two parameters, and τ is a time shift that causes a delay in the state vector.

The estimation equation in time domain is given by (Pederiva, 1992 e Eduardo, 2003):

$$[A][R_{xx}(\tau_i)] + [R_{xx}(\tau_i)][A]^T + [E][R_{nx}(\tau_i)] + [R_{xn}(\tau_i)][E]^T = 0 \tag{7}$$

with

$$[Q] = -\left([E]\left[R_{nx}(\tau_i)\right] + \left[R_{xn}(\tau_i)\right][E]^T \right) = 0 \tag{8}$$

Equation (7) is valid only when the entire state vector is known, which is not possible in practice. In order to overcome this difficulty, the rotor model is reduced by the well-known Guyan model reduction technique so only the measured degrees of freedom df of the rotor are taken into account. In addition, an auxiliary (filter) system is used associated with the measured outputs rotor, whose function is to correlate different time instants, thereby enabling the parameters to be estimated with only a few system outputs. The filter works as illustrated in Fig. 2:

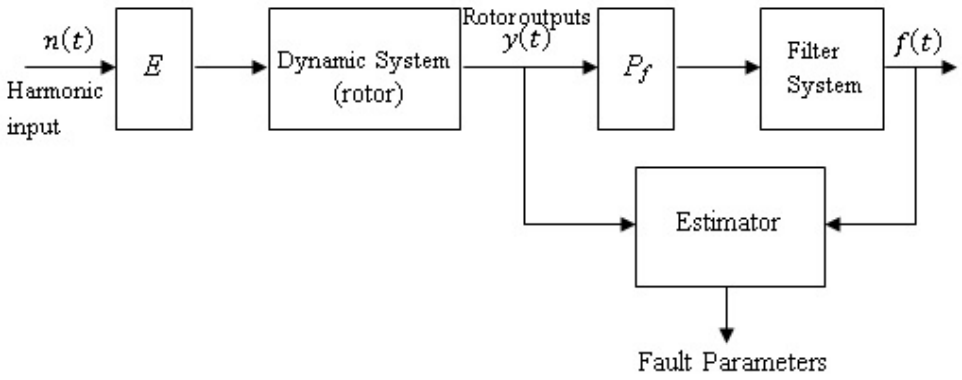

Figure 2. Diagram of the filter actuation

Details about the filter matrices and actuation in the rotor system can be seen in details in Pederiva (1992) and Sanches (2015).

The identification equation in time domain considering only the disk translational *df* is given by (Sanches, 2015):

$$-r_{\eta_3\xi_m} + \left\{ r_{\eta_1\xi_m} \quad \vdots \quad r_{\eta_2\xi_m} \right\} \begin{bmatrix} A_1^{*T} \\ A_2^{*T} \end{bmatrix} = Q_{3_{(1,1:2)}} \tag{9}$$

where Q_3 is a sub matrix of $[Q]$ (Sanches, 2015). η_1, η_2 and η_3 are the filter outputs and ξ_m is the vector of the measured *df*.

3. DESCRIPTION OF THE TEST RIG

The identification equation described by Eq. (9) is applied experimentally to the test rig illustrated in Fig. 3:

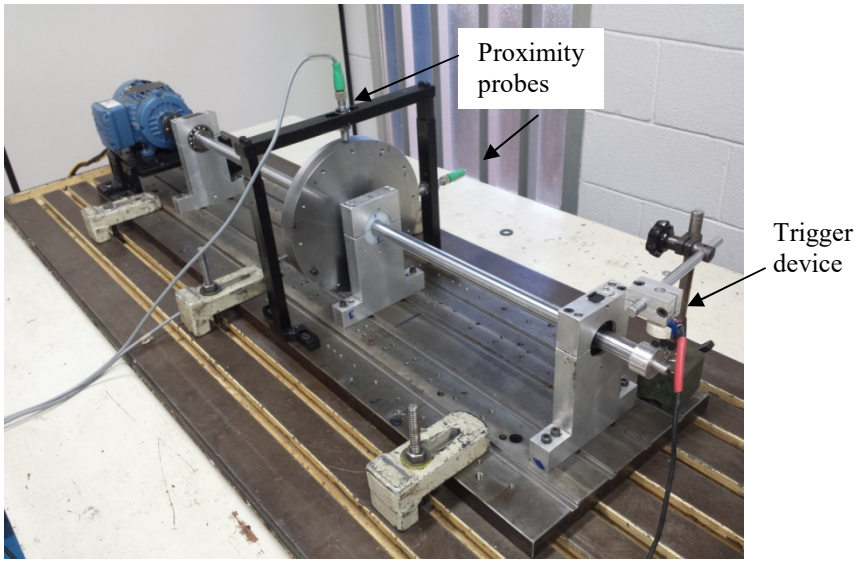

Figure 3. Test rig

This test rig has one disk placed outside of the middle distance between the two rolling bearings. Table 1 describes some of the test rig characteristics:

Table 1. Test rig characteristics

Properties	*Material*	*Inner diameter*	*Outer diameter*	*Mass*	*Thickness*
Shaft	Steel 1045	-	20 mm	2.46 kg	-
Disk	Steel 1020	20 mm	220 mm	7.90 kg	27 mm

The test rig was modeled using finite elements and the shaft was discretized in 11 nodes with a total of 44 degrees of freedom distributed as shown in Fig. 4.

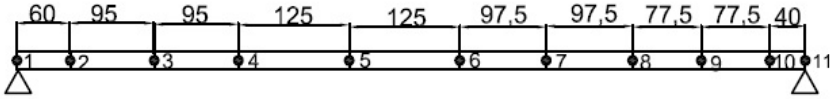

Figure 4. FEM nodes in the test rig – distances in mm

Two *SKF 1205 EKTN9* rolling bearings are placed at nodes #1 and #11 and the disk is located at node #6. A vibration limiter is positioned next to the disk, and the test rig is driven by an AC 0.12 kW electric motor connected to a flexible neoprene coupling located between the motor and the rolling bearing placed at node #1, while a trigger device is positioned at the end of the shaft. The rotation speed is controlled up to the limit of 3600 rpm by a frequency inverter, and the horizontal and vertical disk vibrations are monitored using two proximity probes.

The disk has 12 M5 threaded holes spaced 30° from each other, and the distance d from the center of the holes to the shaft centerline is 98 mm. One of the holes, in which the unbalance is considered at an angle β, is taken as the reference. A mass unbalance m is placed at some specific holes. The unbalance moment, which is calculated by multiplying d and m, and its location (phase) as well as the shaft bow (magnitude and phase) are identified by Eq.(9).

3.1 Identification of rotor parameters

In order to identify the unbalance and shaft bow parameters, it is necessary model that reproduces the dynamic behavior of the machine. The bearing parameters (stiffness and damping), the coupling angular stiffness, and the structural damping, play an important role in the system's physical behavior and should therefore be known before identifying the fault, since they form the matrices $\left[A_1^*\right]$ and $\left[A_2^*\right]$ that are used in the estimation equation given by Eq.(9).

The aforementioned parameters were obtained using the Differential Evolution (DE) optimization technique. The identification procedure consists in comparing the experimental Frequency Response Functions (FRFs) with the numerical (simulated) ones in the non-rotating condition. This condition is assumed considering the bearing parameters remain unchanged with rotation speed.

The experimental FRFs were acquired by placing a shaker on the 4th node and the readings were taken at nodes 2 to 10, making a total of 18 FRFs. Random excitation was used in the horizontal and vertical directions, and the readings were taken in the same directions. The objective function (OF) to be minimized is given by:

$$OF = \sum_{1}^{nf} \frac{\left\| FRF_{\exp,i} - FRF_{sim,i} \right\|}{\left\| FRF_{\exp,i} \right\|} \tag{10}$$

where nf is the total number of FRFs.

Structural damping was modeled as proportional and the optimization results are described in Tab. 2.

Table 2. Identified rotor parameters

Characteristics	*Variables*	*Results*
Bearing	K_{xx}	3.21e6 N/m
	K_{zz}	3.07e6 N/m
	C_{xx}	100.18 Ns/m
	C_{zz}	72.69 Ns/m
Proportional damping	α	2.49
(α[M]+β[K])	β	1.98e-5
Coupling angular stiffness	K_r	589.58 Nm/rad

where *x* and *z* are the horizontal and vertical directions, respectively.

The angular stiffness comes from the flexible neoprene coupling and its value is considered to be equal in both angular coordinates at the node #1.

Figure 5 shows the comparison of experimental and simulated FRFs using the results presented in Tab. 2.

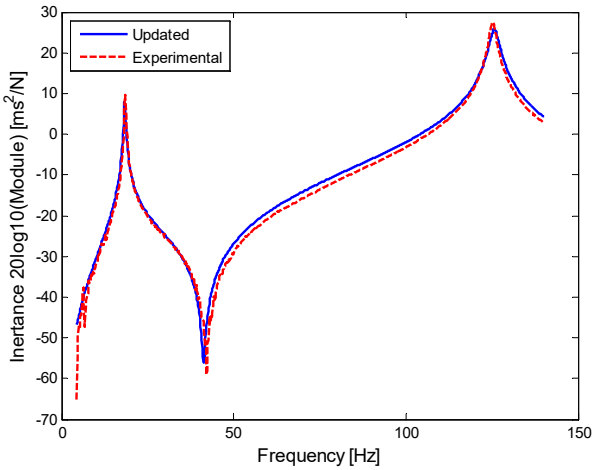

Figure 5. FRF acquired at node #4 – horizontal direction

Based on the results described by Tab(2), the test rig is characterized by the Campbell diagram showed by Fig.6:

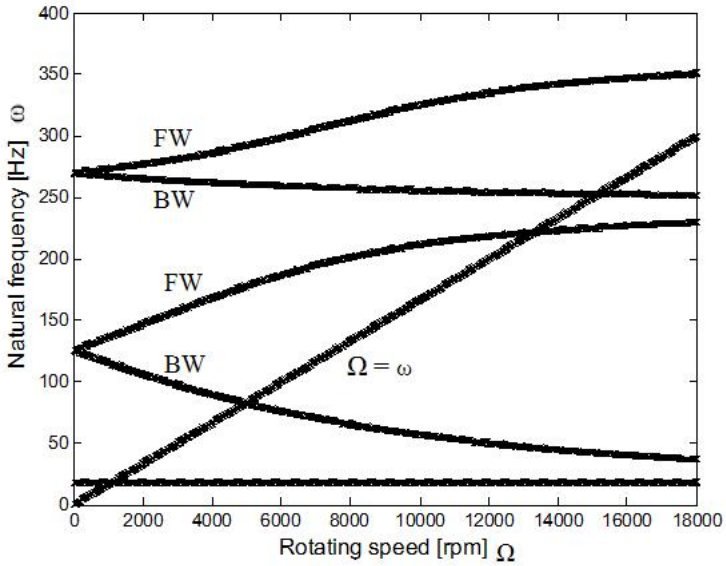

Figure 6. Campbell diagram

4. IDENTIFICATION OF THE UNBALANCE AND SHAFT BOW

The identification procedure is performed experimentally using the test rig showed by Fig.3. An unbalance mass of 4.7 grams is placed at the disk to generate an unbalance moment equal to $4.61.10^{-4}$ kg.m. This unbalance mass is placed in four different positions (phases) in relation to a chosen reference point on the disk/shaft, which coincides with the signal trigger position. Four phases were chosen: $+60^{o}$ (case1), $+150^{o}$ (case 2), $+210^{o}$ (case 3) and $+300^{o}$ (case 4). Each unbalance location (phase) is determine considering the trigger position showed by Fig.(1). The bow magnitude is speed independent and is considered constant, since it depends only on the permanent arching level presented by the shaft.

The reason for choosing four unbalance cases is to test the robustness of the proposed methodology in identifying different unbalance phases as well as determine if the identified shaft bow parameters is really obtained without major deviations

The rotor is considered balanced and the experimental data were acquired at a sampling frequency of 10,000 Hz and a total time of 2s. The identification procedure was performed using five shaft angular frequencies below the first

critical speed: 11, 12, 13, 14 and 15 Hz, and six frequencies above the first critical speed: 23, 24, 25, 26, 27 and 28 Hz. Thus, the dynamics before and above the first critical speed is considered. Only the disk´s responses are used in the identification process given by Eq.(9).

Tables 3 and 4 show the results obtained by the experimental procedure:

Table 3. Identification of the unbalance

Unbalance cases	*Unbalance amplitude* (kg.m)	*Amplitude deviation*	*Phase*	*Phase deviation*
Case 1	3.48e-4	-24.51%	+73.70^o	+22.80%
Case 2	2.45e-4	-46.86%	+191.14^o	+27.43%
Case 3	3.77e-4	-18.22%	+242.26^o	-15.36%
Case 4	3.01e-4	-34.71%	+285.00^o	-5.00%

Table 4. Identification of the shaft bow

Unbalance cases	*Bow amplitude* (μm)	*Phase*
Case 1	44.80	+210.00^o
Case 2	60.24	+197.36^o
Case 3	68.78	+192.32^o
Case 4	52.21	+222.32^o
Mean value	56.51	+205.50^o
Standard deviation	10.33	+13.46^o

Tables 3 and 4 show that the results were obtained with satisfactory convergence, being the shaft bow identified with higher accuracy and minor deviations.

It is worth keeping in mind that shaft bow and unbalance are synchronous with rotor spin, presenting similar symptoms and occurring simultaneously in two different positions of the rotor, thus generating a combined effect that makes it difficult for the identification algorithm to distinguish them from one another in each disk position.

One cause of the discrepancies in the unbalance identification comes from the rotation control system that is not able to maintain the same spin speed of the rotor causing variations in the unbalance magnitude.

Another cause of uncertainties is the existence of a residual unbalance affecting the total disk unbalance as well as its phase. This effect was not taken into account in the experiments.

5. CONCLUSIONS

This paper has shown the results of experimental identification of two simultaneous faults that are synchronous with the machine rotation and present similar symptoms in the rotor vibration. In order to perform this identification, a well-tuned rotor model was necessary to reproduce the machine behavior. The algorithm uses only the system outputs to estimate the fault parameters, using correlation analysis and model order reduction to extract fault information.

The diagnostic strategy used to identify the faults has shown to be able to evaluate severity and, particularly, location (phase) of unbalance and shaft bow.

6. REFERENCES

Chatzisavvas, I. and Dohal, F., 2015. “Unbalance identification using the least angle regression technique”. *Mechanical Systems and Signal Processing*, Vols 50-51, p. 706-717.

Eduardo, A.C., 2003. *Fault Diagnosis in Rotor Systems through Correlation Analysis and Artificial Neural Networks*. Ph.D. Thesis, Faculty of Mechanical Engineer, University of Campinas, Campinas.

Jain, J.R. and Kundra, T.K., 2004. “Model based online diagnosis of unbalance and transverse fatigue crack in rotor systems”. *Mechanics Research Communications,* Vol 31, p. 557-568.

Jalan, A.K. and Mohanty, A.R., 2009. “Model based fault diagnosis of a rotor-bearing system for misalignment and unbalance under steady-state condition”. *Journal of Sound and Vibration,* Vol. 327, p. 604-622.

Lal, M. and Tiwari, R., 2012. “Multi-fault identification in simple rotor-bearing-coupling systems based on forced response measurements”. *Mechanism and Machine Theory,* Vol. 51, p. 87-109.

Lalanne, M., Ferraris, G., 1990. *Rotor Dynamics Prediction in Engineering*, John Wiley and Sons, 1st edition.

Markert, R., Platz, R. and Seidler, M., 2001. " Model based fault identification in rotor systems by least squares fitting". *International Journal of Rotating Machinery*, Vol 7, No 5, p. 311-321.

Nicholas, J.C., Gunter, E.J., Allaire, P.E., 1976. " Effect of residual shaft bow on unbalance response and balancing of a single mass flexible rotor – part 1: unbalance response", *Journal of Engineering for Power*, p. 171-181.

Pederiva, R., 1992, "Identificação Paramétrica de Sistemas Mecânicos Excitados Estocasticamente", Tese de Doutorado, Universidade Estadual de Campinas, Campinas.

Pennacchi, P., Bachschmid, N., Vania, A., Zanetta, G.A., and Gregory, L., 2006. "Use of modal representation for the supporting structure in model-based fault identification of large rotating machinery: part 1 – theoretical remarks". *Mechanical Systems and Signal Processing,* Vol 20, p. 662-681.

Rossner, M., Thuemmel, T., Ulbrich, H., 2015. "Inclusion of unsteady bow in a model-based monitoring system for rotors", *Mechanism and Machine Science: Proceedings of the 9thIFToMM International Conference on Rotor Dynamics* , Vol 21, p.1605-1615.

Sanches, F.D., Pederiva, R., 2011. " Multi faults estimation in rotor systems using correlation analysis". In *Proceedings of the 21stABCM International Congress of Mechanical Engineering – COBEM 2011*, Natal, Brazil.

Sanches, F.D., 2015, "Identificação Simultânea de Desbalanceamento e Empeno de Eixo em Rotores através de Análise de Correlações", Tese de Doutorado, Universidade Estadual de Campinas, Campinas.

Shiau, T.N., Lee, E.K., 1989. "The residual shaft bow effect on dynamic response of a simply supported rotor with disk skew and mass unbalances". *Journal of Vibration, Acoustics, Stress, and Reliability in Design*, p. 170-178.

7. RESPONSIBILITY NOTICE

The authors are the only responsible for the printed material included in this paper.